

Versatile Optical Coherence Tomography system applied for imaging of teeth

Bennett T. Amaechi^{*1}, Adrian Gh. Podoleanu^{a2}, John A. Rogers², Susan M. Highamⁿ³, Shane Dunne⁴, David A. Jackson²

¹Dept. of Community Dentistry, Univ. of Texas Health Science Center, San Antonio, TX 78229, USA; ²Applied Optics Group, School of Physical Sciences, Univ. of Kent at Canterbury, UK;

³Cariology Group, Dept. of Clinical Dental Sciences, Univ. of Liverpool, Liverpool, UK;

⁴Ophthalmic Technologies, Inc., Toronto, Canada.

ABSTRACT

The utility of a versatile multifunctional standalone Optical Coherence Tomography (OCT)/confocal system for imaging dental tissue was investigated. The system can collect A-scan (reflectivity versus depth graph), longitudinal (B-scan) and *en-face* (C-scan) OCT images, simultaneously with a confocal image. The power to the sample was 250 μ W, wavelength $\lambda = 850$ nm and the depth resolution in air was 16 μ m. The OCT images showed caries lesions as volumes of reduced reflectivity. Transversal images (C-scan) showed the *en-face* slices of the tooth tissue like in confocal microscopy. Longitudinal images showed the depth of the lesion into the tooth tissue as well as the different structural layers of sound tooth in the same way as seen in ultrasound images. A-scans performed in locations selected in the *en-face* images provided quantitative data about the reflectivity versus depth. The confocal channel was extremely useful for guidance and it has also shown the integral of the intensity over depth at transversal locations. We concluded that OCT proved capable to detect an early caries lesion, to show the depth of the lesion into the tissue, and quantitatively assess the degree of demineralisation.

Key words: Optical coherence tomography, low coherence interferometry, dental imaging, caries diagnosis, demineralisation, confocal imaging, enamel, dental caries, optical methods

1. INTRODUCTION

For many years radiography^{1,2} has been used for caries diagnosis and restorative decision-making in dentistry. In addition to subjecting patients to ionising radiation, it is neither quantitative nor sensitive enough to detect very early lesions. Early dental caries can be remineralised with therapeutic agents if detected at an incipient stage. The effectiveness of these therapies can only be determined with a method that can quantitatively monitor the change in the mineral status of the caries on a longitudinal basis. Other currently available diagnostic methods such as visual inspection and tactile examination with a probe³ and fibre-optic transillumination^{2,4}, still have limitations in their ability to achieve this goal in that they can only detect caries at a relatively advanced stage and cannot quantitatively assess the mineral status of the lesion. So it seems appropriate to develop a method, which can effectively achieve the above objective without limitations.

Optical Coherence Tomography (OCT) is a new imaging modality, which may be seen as the optical analogue of ultrasound as long as longitudinal images are concerned (images which contain the optical axis, or in ultrasound terminology, B-scan images). It is based on confocal microscopy and low coherence interferometry. The latter is an absolute measurement technique, which allows high-resolution ranging⁵ and characterisation of optoelectronic components^{6,7}. The first application in the biomedical optics field was for the measurement of the eye length⁸. The potential of the technique for high resolution imaging of the tissue is often referred to as optical coherence tomography (OCT)⁹. When applied to medical imaging, OCT is non-invasive, as low powers are used for wavelengths in the therapeutic window 600-1300 nm.

* Correspondence: amaechi@uthscsa.edu; phone: +1 210 567 3200; fax: +1 210 567 4587; www.uthscsa.edu; Dept. of Community Dentistry, Univ. of Texas Health Science Center, San Antonio, TX 78229, USA. ^aA.G.H.Podoleanu@ukc.ac.uk; phone: +44 1227 823272; fax: +44 1227 827558; www.ukc.ac.uk/physical-sciences/aog/Low Cohe/. ⁿsuehigh@liv.ac.uk; phone: 44 151 7065251; fax +44 151 7065937; www.liv.ac.uk

OCT could non-invasively, image the internal microstructures of biological tissues such as tooth¹⁰⁻¹⁴, eye^{15, 16, 8, 17} and skin¹⁷. Numerous reports proved the ability of OCT to provide high resolution images of dental tissues¹⁰⁻¹⁴. However, all previous reports refer to longitudinal OCT imaging only. The information which can be collected cutting the object axially is obviously limited. It would be more natural to see *en-face* slices in the tooth in the way we are used to see them when looking through a microscope. Therefore, we are taking advantage of *en-face* OCT¹⁵ and of combination of the *en-face* OCT technology with confocal microscopy¹⁶, both technologies developed initially for retina imaging, to further the application of the OCT into dental tissue imaging. We investigated the utility of presenting longitudinal (B-scan) as well as *en-face* images (C-scans) from the teeth to detect dental caries.

2. SYSTEM

Any OCT is built around a confocal microscope. However, in the system used in the present study^{16, 18}, a separate confocal channel is provided.

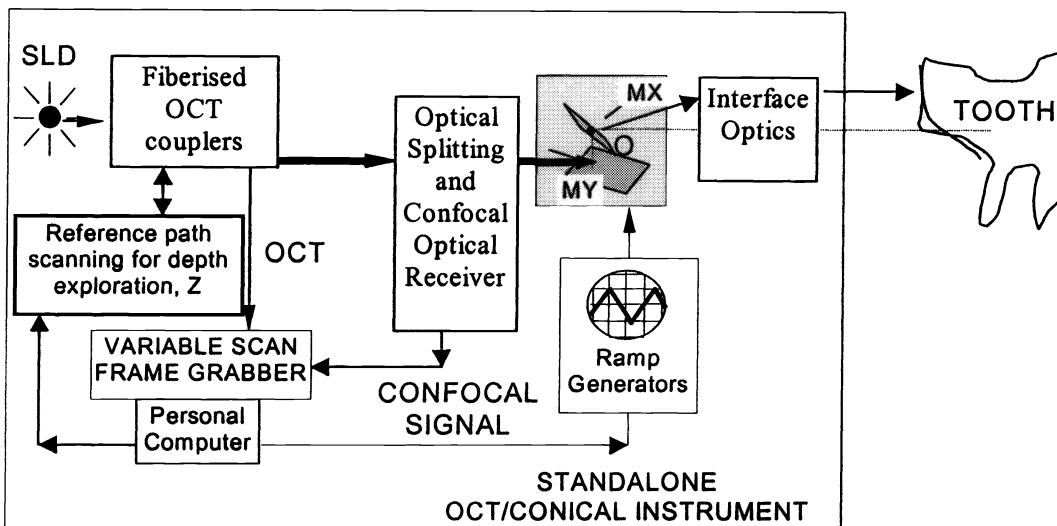


Figure 1. Basic set up of the standalone OCT/CONFOCAL system where a separate confocal receiver diverts parts of the light returned from the tooth. SLD: Superluminescent diode; MX, MY: orthogonal galvanometer mirrors.

The apparatus (Figure 1) comprises an interferometer excited by a pigtailed superluminescent diode (SLD), central wavelength $\lambda = 0.85 \mu\text{m}$, bandwidth $\Delta\lambda = 20 \text{ nm}$, which sends $250 \mu\text{W}$ power to the tooth. The OCT system used was reported elsewhere^{16, 18}, using a configuration of directional single mode couplers. In the sensing arm of the OCT, a splitting device redirects a part of the returned light from the tooth towards a photodetector, behind a lens and a pinhole, used in the confocal receiver. The design is such that the two images, OCT and confocal are in pixel to pixel correspondence.

The OCT and confocal signals carrying the information about reflectivity are applied to a dual input frame grabber, which can display one or both of these signals under the computer control. The frame grabber is synchronised with TTL signals delivered by the two ramps generators controlling the galvanometer pair. For an image size of $3 \text{ mm} \times 3 \text{ mm}$ in the transversal section of the object, the pixel size is $\sim 10 \mu\text{m}$, determined by the numerical aperture of the interface optics. In depth however, the depth resolution in the two channels is different. In the OCT channel, the depth resolution is governed by the spectral properties of the low coherence source, and is half of the coherence length of the source, i.e. $16 \mu\text{m}$. The depth resolution in the confocal channel is $\sim 1 \text{ mm}$, dictated by the interface optic and the optics of the confocal receiver (the numerical aperture of the focusing lens and the pinhole diameter). Both resolutions are the Full Width Half Maximum of the signal profile measured by moving axially a mirror as object, through the focus of the interface optics. The depth resolution of the confocal channel can in principle be improved to a few microns by using a high NA interface optics and a sufficiently small pinhole. However, as long as the OCT channel provides the depth

resolution, the depth resolution in the confocal channel is conceived to be poorer than in the OCT channel. In this way, a very small percentage of the signal reflected by the tooth is sufficient for the confocal channel and the majority of the signal is used in the OCT channel. A large depth of focus allows collection of the OCT signal without the need of dynamic focus¹⁹. If the depth of focus becomes similar to the coherence length, then the focus needs to be moved in synchronism with the translation stage in the OCT channel which determines the position in depth of the scatterer contributing to the OCT signal. This would complicate the system.

In the OCT channel, the signal is proportional to the square of the reflectivity and in the confocal channel to the reflectivity encountered by the scanned beam in the corresponding (x,y) point, integrated over the coherence length in the OCT channel and over the depth of focus in the confocal channel.

The system can operate in different regimes. In the longitudinal OCT regime, only one galvo-scanner of the galvo-scanner pair is driven with a ramp at 700 Hz and the translation stage is moved for the depth range required in 0.5 s. In this case, an OCT B-scan image is produced either in the plane (x,z) or (y,z). The depth range was 1 mm in air for the images presented in this paper. The generation of B-scan images differ from other reports on longitudinal OCT imaging^{6,9} where the B-scan image is constructed out of A-scans (depth profiles of the reflectivity in depth).

In the transversal regime, one galvo-scanner is driven with a ramp at 700 Hz and the other galvo-scanner with a ramp at 2 Hz. In this way, a C-scan image, in the plane (x,y) is generated, at constant depth. Then the depth is changed by moving the translation stage and a new C-scan image is collected. The *en-face* images of caries lesions in the present study were obtained in this way.

Ideally, to collect the reflectivity distribution from the volume of the tooth, the depth interval between successive C-scans should be much smaller than the system resolution in depth and the depth change applied only after the entire C-scan image collected. However, in practice, to speed up the acquisition, the translation stage was moved continuously at a low speed, of 50 $\mu\text{m/s}$. For the 2Hz frame rate this means 25 μm between the frames, a slightly larger value than the depth resolution. In this way, 40 pair-frames from a volume in depth of 1 mm in air are acquired in 20 s.

The confocal image was useful for identifying the lesions, aligning the tooth and evaluating the overall map of reflectivity along X or Y axis in the longitudinal regime or in the plane (x,y) in the transversal regime. In the longitudinal regime, the confocal image shows little variation in depth due to the large depth of focus used. However, the confocal channel may be very useful *in vivo*, when lateral movement of the patient in the scanning direction X or Y respectively picked up from the confocal image can be used to correct the OCT image.

3. METHODOLOGY

Fifteen freshly extracted bovine incisor teeth free from caries, cracks or enamel malformations were selected and polished with pumice slurry to remove organic contaminants from the labial surface. The teeth were then painted with two coats of a non-fluorescent acid-resistant colourless nail varnish, except for an exposed window (2 mm x 2 mm) on the labial surface of the teeth. Caries-like lesions were then produced on each window by demineralisation of the teeth in acidic buffer solutions containing 2.2mM KH_2PO_4 , 50mM acetic acid, 2.2mM of 1M CaCl_2 and 0.5ppm fluoride, at a pH of 4.5²⁰. Prior to demineralisation (bd) and following 3-day demineralisation (ad), A-, B-, and C-scan OCT images of each tooth involving the window area were recorded. The OCT images were acquired as described in previous publications^{15, 16}. The A-scan shows the depth (mm) resolved reflectivity (dB) of the tooth tissue and therefore was used to calculate the degree of reflectivity, R (dB.mm) of the tissue at any depth, as described by Amaechi *et al.*²¹.

3. RESULTS

A pair of *en-face* OCT image and confocal image is displayed in Figure 2. Longitudinal OCT images, hardware produced by switching the system to the B-scan regime, are presented in Figures 3 and 4. Both the transversal (*en-face*) and longitudinal images showed the caries lesion as volumes of reduced reflectivity. The caries appears as bright in the confocal image. The confocal image shows an integral of the reflectivity over a large depth, 1 mm and therefore the high reflectivity of the superficial layer is expected to dominate any confocal variations in depth.

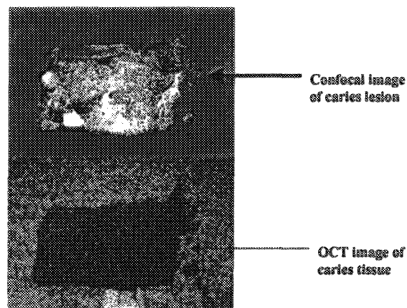


Fig. 2. Single frame of OCT and confocal images. Lateral size: 5 mm x 5 mm.

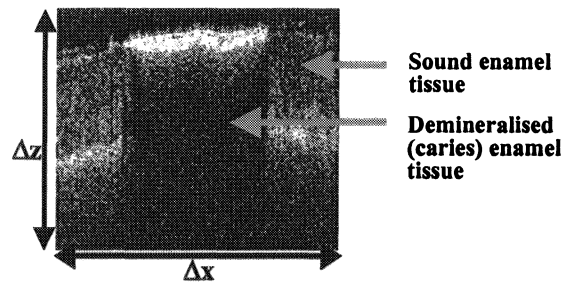


Fig. 3. Longitudinal OCT image from the middle of the transversal image in figure 2 showing a caries lesion. $\Delta X = 5$ mm, $\Delta z = 0.6$ mm.

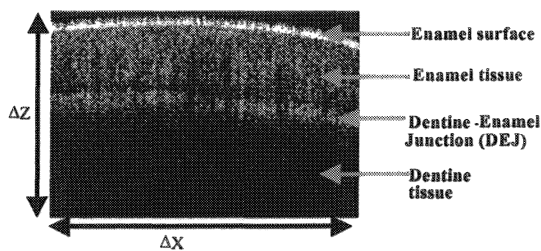


Fig. 4. Longitudinal OCT image from the sound part of the tooth in figure 2. This corresponds to a cut at the beginning of exploration of the stack along Y, stopped at $\Delta Y = 0.1$ mm, $\Delta z = 0.6$ mm.

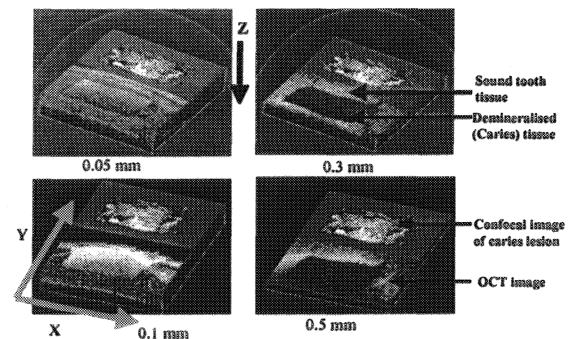


Fig. 5. Stack of 42 pairs of OCT and confocal images viewed at different depths, as indicated below each frame. Lateral size: 5 mm x 5 mm.

42 frames containing both the OCT and confocal images were collected at 2 Hz. Then a stack of images (Figure 5 and 6) was constructed. Using a specialised software program, the stack can be explored in any directions, X, Y or Z. Figure 6 shows sections in the stack at different depths. Here the confocal image was used more for guidance, as the depth information is in the OCT image. The 3D display shows the transversal appearance as well as longitudinal OCT images. Clicking on any of the faces of the stack, an exploration perpendicular on that face could be displayed. The transversal images show the *en-face* slices of the tooth tissue (including both sound and carious areas) from the tooth surface up to the maximum penetration depth (Figures 5 and 6). Due to the inclination of the object in relation to the optic axis, the transversal images display sections similar to the longitudinal images. The superior guidance allowed by the confocal channel as well as the views offered by the 3D display of stack of images allows precise selection of the (X,Y) point where an A-scan should be performed. Such A-scans could be either inferred from the stack of images or collected hardware. Demineralisation of the tooth tissue is seen on the images as a decrease in reflectivity. An A-scan graph (Figure 7) showed the levels of reflectivity (dB) versus depth (mm) of penetration into the tooth tissue. The decrease in reflectivity of the tooth tissue following demineralisation manifested in A-scan as reduction in the area under the graph (Figure 8). Quantitative analysis from the A-scans²¹ also confirmed the reflectivity loss following demineralisation. Statistical analysis (paired t-test, $\alpha=0.05$) showed that the mean value of degree of reflectivity, R (dB.mm), after 3 days demineralisation (4.32 ± 2.72) was significantly (probability $p<0.005$) less than before demineralisation (31.86 ± 9.30).

The same internal structure as seen in the longitudinal images in Figures 3 and 4 could be noticed in the OCT images in Figure 5, 6 and 7. The layers identified in Figures 3 and 4 are clearly displayed in these images, although the OCT cuts (C-scans) are oriented perpendicular to the Z direction.

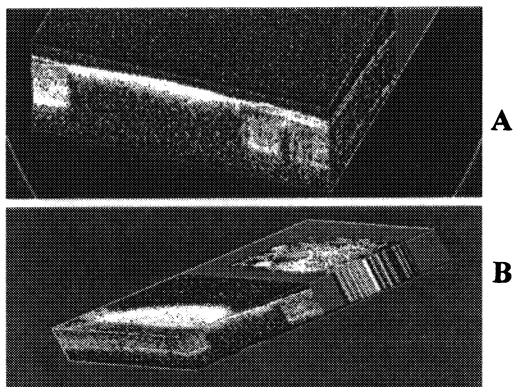


Fig. 6. Lateral views of the stack in figure 5. White means higher reflectance and comes from the sound parts of the tooth. A: Stack in figure 5 after exploration along Y, stopped at $Y = 2.5$ mm (middle of the tooth), showing a longitudinal slice in the plane (X,Z), which displays the X extension of the cavity; B: Stack in figure 5 explored along X and Y, stopped at $X = 3$ mm, $Y = 0.2$ mm, which shows the Y extension of cavity in the plane (Y,Z) and longitudinal OCT image in the plane (X,Z) in the sound tissue.

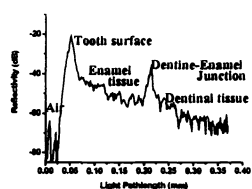


Fig. 7. A-scan graph demonstrating the different structural layers in a sound tooth tissue in the middle of the image in figure 5.

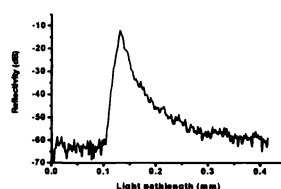


Fig. 8. A-scan graph demonstrating the decrease in reflectivity of the tooth tissue following demineralisation. This manifested in A-scan as reduction in the area under the curve.

4. DISCUSSION

The present study demonstrated that OCT can perform high resolution cross sectional imaging of the internal structure of the tooth *in vitro* and in real time, and it is believed that it can do same *in vivo* and *in situ*.

When in transversal regime, *en-face* images collected at different depths are subsequently used to reconstruct 3D volumes of the tissue. The reconstruction allows software inferred OCT longitudinal images at any transversal position in the stack. The position in depth in the stack before creating longitudinal OCT images is also adjustable, offering a valuable guidance tool for exploring the 3D volume of the tissue. This is illustrated by movies showing either depth or lateral exploration along one of two possible different directions in the stack of transversal OCT images. The system, equipped with the 3D rendering feature, acts as a valuable diagnostic tool allowing “peeling off” of transversal and longitudinal biologic material to investigate different internal features. The confocal image can also be displayed sideways, along with the *en-face* OCT image at each depth. The software allows the reconstruction of the 3D profile to be seen from different angles. The longitudinal image (Figures 3) showed the depth of the demineralisation (caries) inside the tooth tissue, thereby proving OCT to be a potential tool for decision-making in restorative dentistry, since the decision to remineralise or restore a caries lesion depends on the depth of the lesion into the tooth.

The ability of OCT to detect an incipient caries lesion was successfully demonstrated in the present study. OCT was able to discriminate between sound and demineralised (cariou) tooth tissue by their differences in reflectivity; depicting carious tissue as volumes of reduced reflectivity (Figures 2, 3, 5 and 6). The system is presently being developed to use

reflectivity, polarisation and birefringence to discriminate between sound and demineralised tissue. The result of the present study demonstrated that OCT would be a suitable tool for routine examination in the dental clinic. It would also be applicable in an *in vivo*, *in situ* or *in vitro* testing of the efficacy of products formulated to inhibit demineralisation and/or promote remineralisation. Amaechi *et al.*¹³ have demonstrated the use of A-scan from OCT imaging to produce a quantitative data relating to the degree of change in reflectivity, and hence the degree of change in mineral level, of the tooth tissue following development of caries. The provision of quantitative data as well as giving information regarding depth, all without dangerous ionising radiation, gives OCT superiority over the conventional x-ray technology which has been the tool for caries diagnosis for many years.

5. CONCLUSIONS

The present investigation demonstrated the utility of an OCT system which can show C-, B-, and A-scan images of the tooth tissue. Such an instrument can be a useful tool to both dentists and dental researchers. On examination of a tooth, the compounding information in rectangular directions, transversal and axial, allows better diagnosis than when using longitudinal OCT imaging only. Successive displays of transversal and longitudinal cuts at different positions in the 3D stack of en-face OCT images give a direct view of the caries volume. A-scan remains the best mode for quantitative analysis of the activity (demineralisation or remineralisation) of the caries lesion over time, and therefore could be exploited in the determination of the effect of caries therapeutic agents (e.g. fluoride mouthrinse, fluoride dentifrice) or laboratory testing of a new oral healthcare product. However, the 3D imaging mode demonstrated here helps in choosing the position of the A-scan in transversal section.

It is concluded that OCT could detect an early caries lesion, show the depth of the lesion into the tissue, and quantitatively demonstrate the degree of demineralisation. Hence, it has the potential of detecting obscured caries such as caries underneath dental plaques, dental restorations and gum, and may possibly replace the conventional dental radiograph to eliminate the danger of hazardous ionising radiation.

ACKNOWLEDGEMENT

The authors acknowledge the support of the Engineering Physical Sciences Research Council of the UK and Ophthalmic Technologies Inc., Canada.

REFERENCES

1. A. Wenzel, M. J. Larsen, and O. Fejerskov, "Detection of occlusal caries without cavitations by visual inspection, film radiographs, xeroradiographs, and digitized radiographs". *Caries Res* **25**, pp. 365-371, 1991.
2. A. Wenzel, E. H. Verdonshot, G. J. Truin, and K. G. König, "Accuracy of visual inspection, fibre-optic transillumination, and various radiographic image modalities for the detection of occlusal caries in extracted non-cavitated teeth". *J. Dent. Res.* **71**, pp. 1934-1937, 1992
3. K. R. Ekstrand, I. Kuzmina, L. Bjørndal, and A. Thylstrup, "Relationship between external and histologic features of progressive stages of caries in the occlusal fossa". *Caries Res* **29**, pp. 243-250, 1995.
4. A. Schneiderman, M. Elbaum, T. Shulz, S. Keem and M. Greenebaum, "Assessment of dental caries with digital imaging fibre-optic transillumination (DIFOTTTM): In vitro study". *Caries Res* **31**, pp. 103-110, 1997.
5. S. A. Al-Chalabi, B. Culshaw and D. E. N. Davies, "Partially coherent sources in interferometric sensors", *First International Conference on Optical Fibre sensors*, 26-28 April 1983, I.E.E. London, pp. 132-135, 1983.
6. R. C. Youngquist, S. Carr, and D. E. N. Davies, "Optical coherence-domain reflectometry: A new optical evaluation technique," *Opt. Lett.* **12**, pp. 158-160, 1987.
7. H.H. Gilgen, R. P. Novak, R. P. Salathe, W. Hodel, P. Beaud, Submillimeter optical reflectometry", *Lightwave Technol.* **17**, pp.1225-1233, 1989.
8. A.F.Fercher and E.Roth, "Ophthalmic laser interferometry", *Proc. SPIE* **658**, pp. 48-51, 1986
9. D. Huang, E.A. Swanson, C. P. Lin, J. S. Schuman, W. G. Stinson, W. Chang, M. R. Hee, T. Flotte, K. Gregory, C. A. Puliafito and J. G. Fujimoto, 'Optical coherence tomography', *Science* **254**, pp. 1178-1181, 1991.
10. B. W. Colston, Jr., M. J. Everett, L. B. DaSilva L. L. Otis, P. Stroeve, and H. Nathel. "Imaging of hard- and soft-tissue structure in the oral cavity by optical coherence tomography". *Appl Opt* **37**; pp. 3582-3585, 1998.

11. F. I. Feldchtein, G. V. Gelikonov, V. M. Gelikonov, R. R. Iksanov, R. V. Kuranov, A. M. Sergeev, N. D. Gladkova, M. N. Ourutina, J. A. Warren, Jr., and D. H. Reitze "In vivo OCT imaging of hard and soft tissue of the oral cavity". *Opt. Express*, **3**, pp. 239-250, 1998.
12. A. Baumgartner, S Dichtl, CK Hitzenberger, H Sattmann, B. Robl, A Moritz, Fercher AF, and W. Sperr,. "Polarisation-sensitive optical coherence tomography of dental structures". *Caries Res* **34**; pp. 59-69, 2000.
13. A. Baumgartner, CK Hitzenberger, S Dichtl, H Sattmann, A Moritz, W. Sperr, and Fercher AF. "Optical coherence tomography of dental structures". *Proc Spie* 3248; pp. 130-136, 1998.
14. B.W.Colston, Jr., U. S. Sathyam, L. B. DaSilva and M.J.Everett, P. Stroeve, L. L. Otis, "Dental OCT", *Opt. Express* **3**, pp. 230-238, 1998
15. A. Gh. Podoleanu, M. Seeger, G. M. Dobre, D. J. Webb, D. A. Jackson and F. Fitzke "Transversal and longitudinal images from the retina of the living eye using low coherence reflectometry," *J. Biomed Optics*, **3**, pp. 12-20, 1998.
16. A.Gh. Podoleanu and D. A. Jackson, "Combined optical coherence tomograph and scanning laser ophthalmoscope", *Electron. Lett.* **34**, pp. 1088-1090, 1998.
17. A. Gh. Podoleanu, J. A. Rogers, D. A. Jackson, and S. Dunne "Three dimensional OCT images from retina and skin" *Opt. Express* **7**, pp. 292-298 2000.
18. A. Gh. Podoleanu and D. A. Jackson, "Noise Analysis of a combined optical coherence tomography and confocal scanning ophthalmoscope," *Appl. Opt.*, **38**, pp. 2116-2127, 1999.
19. A.Gh. Podoleanu, J. A. Rogers, and D. A. Jackson, "Dynamic focus applied for correct determination of flow speed of a biological liquid using OCT", *Proc. SPIE* 3746, B. Y. Kim, K. Hotate eds., OFS-13, Intern Conf. on Optical Fiber Sensors, April 12-16, 1999, Kyongju, Korea, pp. 288-291.
20. B. T. Amaechi, S. M. Higham, and W. M. Edgar, "Factors affecting the development of carious lesions in bovine teeth *in vitro*". *Arch. Oral Biol.* **43**, pp.619-628, 1998
21. B. T. Amaechi, S. M. Higham , A. Gh. Podoleanu., J. A. Rogers, and D. A. Jackson "Use of Optical Coherence Tomography for assessment of dental caries: quantitative procedure". *J. Oral Rehab.* **28**, 2001 (In press).